Ultrasound Tomosynthesis: A New Paradigm for Quantitative Imaging of the Prostate

Fereshteh Aalamifar[1,2(✉)], Reza Seifabadi[2], Marcelino Bernardo[2],
Ayele H. Negussie[2], Baris Turkbey[2], Maria Merino[2], Peter Pinto[2],
Arman Rahmim[1], Bradford J. Wood[2], and Emad M. Boctor[1]

[1] Johns Hopkins University, Baltimore, MD, USA
fereshteh@jhu.edu
[2] National Institutes of Health, Bethesda, MD, USA

Abstract. Biopsy under B-mode transrectal ultrasound (TRUS) is the gold standard for prostate cancer diagnosis. However, B-mode US shows only the boundary of the prostate, therefore biopsy is performed in a blind fashion, resulting in many false negatives. Although MRI or TRUS-MRI fusion is more sensitive and specific, it may not be readily available across a broad population, and may be cost prohibitive. In this paper, a limited-angle transmission US methodology is proposed, here called US tomosynthesis (USTS), for prostate imaging. This enables quantitative imaging of the prostate, such as generation of a speed of sound (SOS) map, which theoretically may improve detection, localization, or characterization of cancerous prostate tissue. Prostate USTS can be enabled by adding an abdominal probe aligned with the transrectal probe by utilizing a robotic arm. In this paper, we elaborate proposed methodology; then develop a setup and a technique to enable *ex vivo* USTS imaging of human prostate immediately after prostatectomy. Custom hardware and software were developed and implemented. Mock *ex vivo* prostate and lesions were made by filling a mold cavity with water, and adding a plastisol lesion. The time of flights were picked using a proposed center of mass method and corrected manually. The SOS map with a difference expectation-maximization reconstruction performed most accurately, with 2.69 %, 0.23 %, 0.06 % bias in estimating the SOS of plastisol, water, and mold respectively. Although USTS methodology requires further ex vivo validation, USTS has the potential to open up a new window in quantitative low-cost US imaging of the prostate which may meet a public health need.

Keywords: Transmission ultrasound · Ultrasound tomography · Ultrasound tomosynthesis · Robotic ultrasound · *Ex vivo* · Prostate

1 Introduction

Prostate cancer is the most common male cancer in the United States with an estimated 220,000 new cases and 28,000 deaths in 2015 [1]. A key to survival and to avoid over-treatment is early detection, and accurate characterization [2]. Systematic sextant biopsies under TRUS guidance have been the gold standard technique since the 1980's [3]. TRUS is real-time, relatively low cost, and shows the prostate capsule and

boundaries. However, it suffers from poor spatial resolution, subjectivity, and low sensitivity for cancer detection (40–60 % [4]).

MRI is the superior imaging modality for visualizing prostate gland, nerve bundles, and clinically-relevant cancer. However, real-time MRI is challenging, requires specialized costly equipment, and in-gantry prostate biopsy is time and resource intensive and impractical to apply across a broad population. Fusion of TRUS and multi-parametric MRI takes advantage of the strengths of both imaging modalities. In fusion-guided biopsy, targeting information is solely dependent on MR images [4]. Even though US-MRI fusion guided biopsy has shown to be highly sensitive to detect higher-grade cancer, it still suffers from high false positives for lower-grade cancers resulting in unnecessary biopsies [4]. Also, MRI is expensive and less available to the broad population.

Some US based technologies have recently been proposed to address this clinical need in addition to MRI-US fusion, including elastography [5], doppler, and US tissue characterization [6]. Although several studies reported significant improvement in prostate cancer identification with quasi-static elastography, there are still some limitations in reproducibility, subjectivity, and the inability of this method to differentiate cancer from chronic prostatitis [5]. Time series analysis [6] is an interesting new machine learning technique to perform the tissue characterization and has recently shown promising results for marking cancerous areas of prostate using the US RF image [6]. This machine learning method is still based on a post-processing of reflection data.

Transmission ultrasound imaging works based on transmission of US signals. The received signal can be used to reconstruct the volume's acoustic properties such as SOS, attenuation, and spectral scattering maps. This information may theoretically be able to differentiate among different tissue types, including cancerous tissues. Transmission ultrasound can be performed in two ways: full angle and limited angle, just as with tomography. Full angle is a described technique called ultrasound computed tomography which has been extensively used for breast imaging [7] and recently, imaging of extremities [8]. Limited angle, however, is a relatively more recent technique, which has also been used in breast imaging [9]. Similar to X-ray tomosynthesis (which is a limited angle version of CT [computed tomography]), here, we refer to the limited angle US tomography as "US tomosynthesis" (USTS).

The current transmission US systems (e.g. [7, 8]) only work with breast, since it is an easy target to scan in a small water tank. Leveraging these recent findings, we propose a method to further this technology to prostate cancer diagnosis and screening utilizing robotic technology. In this concept (Fig. 1), a bi-plane or tri-plane TRUS probe resides in the rectum, and a linear/curved array transducer resides on the abdomen/pelvis, using the bladder as an acoustic window to the prostate. The abdominal probe can be fixed and aligned with the TRUS probe using a co-robotic setup similar to the one proposed in [10]. *Ex vivo* modeling is requisite prior to evaluating prostate USTS *in vivo*. The first step is to evaluate the feasibility of USTS in prostate cancer detection in a controlled benchtop environment, to understand the potential of this technology. Therefore, this paper focuses on modeling and developing a system and method for *ex vivo* prostate USTS. The system was evaluated with a mock prostate and lesions with comparable SOS.
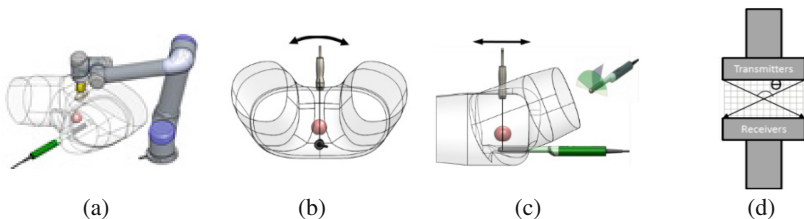
Fig. 1. (a) Prostate ultrasound tomosynthesis concept: a bi/tri-plane TRUS probe is placed into the rectum and a linear/curved array transducer is placed on patient's abdomen; (b) sagittal USTS imaging, (c) axial USTS imaging. (d) USTS image reconstruction concept; larger angel Θ leads to more tomographic data, and less artifact in the reconstructed image.

2   Method

2.1   System Components

For the *ex vivo* study, we propose a setup as depicted in Fig. 2. In this setup, two 128 arrays, 6 cm, linear US probes are precisely aligned. It should be noted that in the *in-vivo* study a transrectal probe which has similar geometry to the abdominal probe used in this setup can be utilized (e.g. Ultrasonix BPL9-5/55). The distance between the probes is adjustable to provide sufficient acoustic window with contact against the scanned volume. The *ex vivo* prostate can be put inside a patient-specific, 3D printed, US friendly mold, whose 3D geometries are based upon 3D MRI data. This mold is placed inside a container which has transparent rubber windows. Small amount of acoustic-transmitting liquid is injected to fill the gaps between the prostate, mold, and container. The container is placed between the aligned probes and its height is adjusted in order to scan different slices.
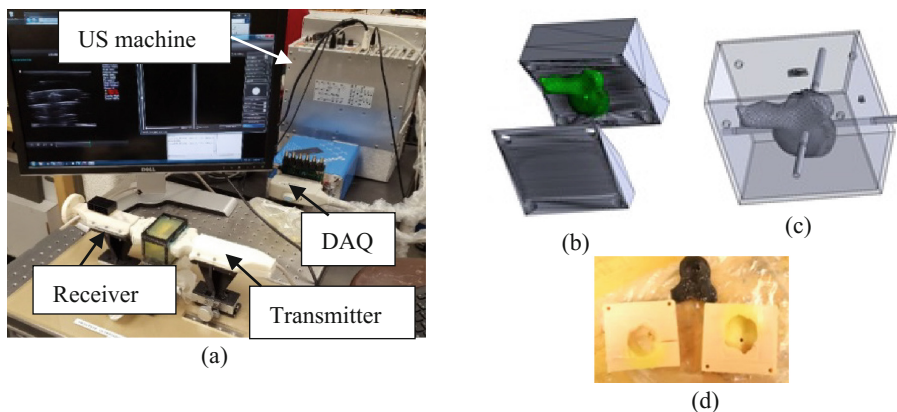

Fig. 2. (a) USTS *ex vivo* setup, The patient specific molds to correspond MRI, histology, and USTS slices. (b) The 3D printed mold for MRI-histology comparison. (c) The 3D printed box used to create the US friendly mold. (d) The US friendly mold and the 3D printed prostate with its seminal vesicles.

MRI and histology are the ground-truths for comparison of the USTS image reconstructed using this setup. The technique and test bed model were designed to enable direct correlation with MRI and matching slices of correlative histology whole mounts. This technique was performed in two steps: first, a patient specific mold (as shown in Fig. 2b) with grooves to guide histology knife is 3D printed. The grooves are 3 or 6 mm apart and result in histology slices specifically custom designed to correspond to MR image slices [11]. Second, the same mold is created using an US friendly material with marks indicating the corresponding slices to be scanned using the US probes.

The US friendly mold was made from acrylamide gel with 1523 m/s SOS and other relevant tissue mimicking property as reported previously [12]. The phantom does not decay, is rigid enough to hold the prostate, and has appropriate SOS suitable for reconstruction (will be described later). In order to make the mold, initially the prostate (with seminal vesicles) is segmented from the clinical MR image. This prostate volume is saved as a stereolithography (.stl) file and printed using a 3D printer (uprint, Stratasys). The 3D printed prostate is positioned inside a box at similar position and orientation compared to MRI 3D printed mold using guide rods as shown in Fig. 2c. Then, the acrylamide solution was poured into the box. After solidification, the rods were removed and the mold was cut to remove the 3D printed prostate. Figure 2d shows the US friendly mold. The prostate can be put inside the mold cavity and the mold's halves are adhered together. Then, the mold is inserted into a container. The container holds the mold in place during the USTS scan, can be filled with liquid to fill the acoustically insulating air gaps between mold and prostate, and provides windows made of mylar sheet to provide US transparency. The container is marked with lines that determine the slices that correspond to the MRI slices.

We used two linear array Ultrasonix probes. The transmitting probe was connected to an Ultrasonix Sonixtoch scanner (Vancouver, BC). As shown in Fig. 2a, the receiving probe was connected to an Ultrasonix Data Acquisition (DAQ) device, which can receive the US waveforms of 128 channels in parallel with sampling frequency of 40 MHz.

2.2 Data Processing

In this study we were interested in SOS in each pixel of the image (as shown in Fig. 1d). To reconstruct an USTS image, i.e. to calculate the SOS in each pixel of the image, two pieces of information are required: the accurate distances between each transmit-receive pair, and the measured time of flight (TOF) between them.

The US data collected contains 128 waveforms per transmitter, each corresponding to one receiver; and one image (slice) is calculated from 128 transmissions. Hence, in order to compute the SOS, the TOF should be picked at all 128×128 (=16384) waveforms. A MATLAB interface was implemented to pick the TOFs semi-automatically. The initial locations of the TOFs were estimated using a center of mass method as:

$$t_{cm} = \frac{\int_t t s^2(t) dt}{\int_t s^2(t) dt} \qquad (1)$$

where *s(t)* is the intensity of the received signal at time *t*. *s(t)* is set to zero outside
$[t_{\text{bg}}-w, t_{\text{bg}} + w]$, where t_{bg} is the estimated background TOF, and *w* is half of a certain
window length to reduce the effect of noise and refractions. As shown in Fig. 3, some
of the waveforms contained electrical noise, or refracted delayed signals which could
result in miss-selection of the TOF. The MATLAB interface allows the user to correct
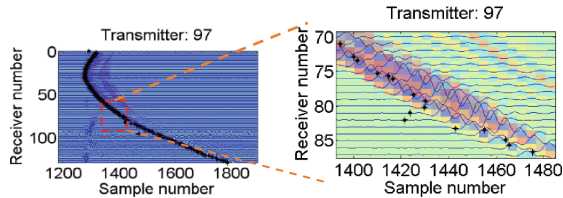for these miss-selections.

Fig. 3. A sample of raw data.

The grid area between transmit-receive pairs (Fig. 1d) were formulated as a system
matrix and the following equation was used to calculate the image based on straight-ray
US propagation approximation [10]:

$$S(X - X_{bg}) = T - T_{bg} \qquad (2)$$

Where *S* is the system matrix, *X* is a vectored concatenation of the image matrix,
and *T* is a vector containing the TOF measurements. X_{bg} and T_{bg} are the known
background SOS values, and the measured TOFs for background respectively. The
background image was collected by scanning a slice that only contains the acrylamide
gel. This information helps in compensating for probes' misalignment and measure-
ment bias [10]. Equation (2) is under-determined and would be computationally
expensive to solve analytically. Hence, we tested two iterative methods of conjugate
gradient and expectation maximization. Since the background information is incor-
porated, these methods are referred to as Diff-CG and Diff-EM in the results. More
details regarding the Diff-EM method could be found in [13].

2.3   Simulation Setup

A simulation study was carried out to answer the following questions for the designed
setup: (1) How well the image can be reconstructed given the limited angle data and the
small difference between cancerous and non-cancerous SOS [14]; (2) What is the best
SOS for the background material (i.e. which material should be chosen for the
US-friendly mold). It should be noted that this study simulates the mathematics of
the reconstruction problem without considering US wave propagation properties. The
locations of probes was simulated on top and bottom of the image with 5 cm axial
distance. The ground-truth image was created with arbitrary features based on the

typical size of the prostate and lesions. As shown in Fig. 4a, the prostate can be modeled as a 3 × 4 cm ellipse and contains two lesions of size 5 and 10 mm in diameter. The speeds of sound in prostate are set to 1614 m/s for prostate region and, 1572 m/s and 1596 m/s for the two lesions based on [14].

2.4   Phantom Study

Using the setup shown in Fig. 2, an image of the mock prostate was acquired. The US machine was set in B-mode image acquisition mode with depth of 7 cm, US frequency of 5 MHz, and aperture size equal to 1 (equivalent to 2 elements in Ultrasoix machine) to enable sequential transmission of US waves. Mock *ex vivo* study was performed by filling the mold cavity with water (1480 m/s) and attaching to the inner part of the mold a lesion made of plastisol ($\sim$1375 m/s). The container with the mold inside was placed between the aligned probes and their axial distance was adjusted using a caliper to 50 mm. US gel was applied to the probes' tip to enhance the coupling and the center slice was chosen to do USTS data collection.

3   Results

3.1   Simulation Results

A simulation phantom was created in MATLAB based on the prostate description given above. As shown in Fig. 4, a background speed of 1523 m/s (similar to general tissue speed of sound) produced a superior image than ones with 1375 m/s and 1010 m/s, corresponding to plastisol and silicon ecoflex respectively. Artifacts in the images are due to the limited angle data but, the lesions are still distinguishable from the prostate.
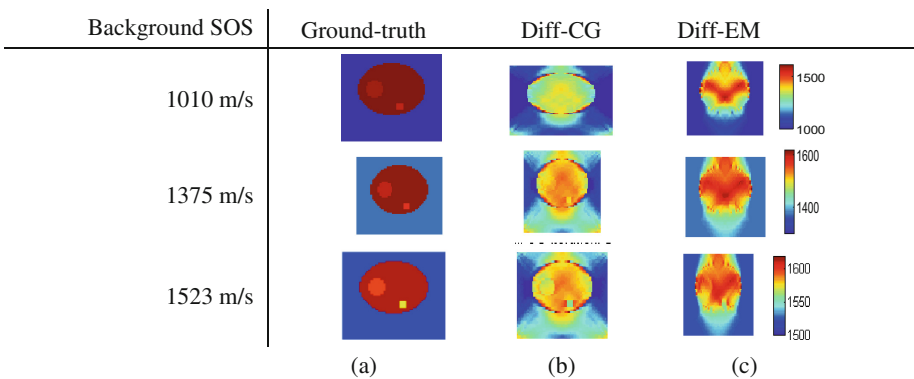

Fig. 4. Simulation results: (a) ground-truth simulation phantoms; (b–c) reconstructed SOS map using (b) Diff-CG and (c) Diff-EM methods.

3.2   Phantom Results

Figure 5a shows a B-mode image of a slice of the mock prostate. The TOF was picked once automatically, and once with manual correction; then the image was reconstructed. Images using Diff-CG and automatically picked TOF contained a high amount of artifacts that increased with number of iterations. The Diff-EM method with manually corrected TOF produced the most accurate results, with the least amount of artifacts, and is shown in Fig. 5c. The theoretical SOSs are around 1523, 1480, and 1375 m/s for mold, water, and plastisol respectively and as shown in the Fig. 5c, these values in one pixel in each of these areas are estimated as 1523, 1476, and 1415 m/s. Table 1 shows bias and noise for a 5 × 5 group of pixels around each of these pixels for the different methods. Diff-EM method seems less robust to TOF error while Diff-CG was less robust to other experimental noise and errors.

Table 1. Bias and noise in the reconstructed images using the two methods at different iterations.

Iteration	Diff-CG				Diff-EM			
	Auto TOF pick		Corrected TOF		Auto TOF pick		Corrected TOF	
	20	50	20	50	20	50	20	50
%Bias^p	2.89	3.68	3.44	4.1	1.77	16.5	2.93	2.69
%Bias^w	0.86	1.30	0.38	0.95	0.79	3.47	0.29	0.23
%Bias^b	0.80	1.52	0.79	1.42	0.06	0.20	0.11	0.06
Noise	15.7	30.5	14.10	27.05	1.06	4.57	1.20	1.14

^{p}: plastisol; ^{w}: water; ^{b}: background. Noise was calculated as the standard deviation of background pixels.
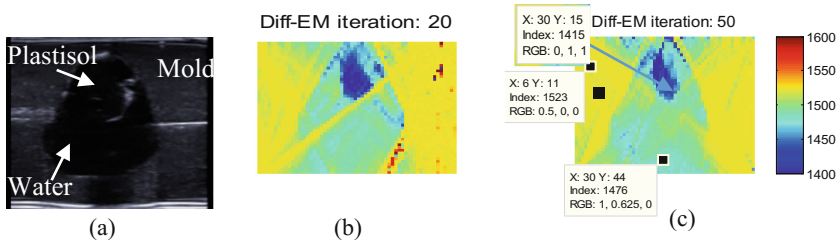

Fig. 5. (a) B-mode image, (b–c) Reconstructed image using Diff-EM method and (b) automatically picked TOF (more iterations causes more artifacts), and (c) manually corrected TOF.

4   Conclusions

In this study, we proposed and modeled a new paradigm for quantitative imaging of prostate, that we call ultrasound tomosynthesis. Prostate cancer screening, biopsy, focal image guided therapies, and brachytherapy are examples of the clinical applications that could potentially integrate this technology. In this study, a setup and a technique

were developed to evaluate feasibility of prostate USTS in *ex vivo* prostate taken from prostatectomy patients. Simulation and phantom studies were done to evaluate the feasibility of this setup. The proposed setup could be used for patient-specific USTS study of *ex vivo* tissues. The SOS map reconstructed from a mock *ex vivo* prostate with relevant acoustic properties showed promise. Immediate next step includes *ex vivo* study. Since the SOS contrast among different tissues may be small in prostate, the attenuation map and more advanced reconstruction techniques including regularization [15] will be investigated. There is a critical public health need for improved methodologies of prostate tissue characterization and prostate cancer detection that are cost-effective, broadly accessible, and easy to use.

References

1. Siegel, R., et al.: Cancer statistics. Cancer J. Clin. **64**, 9–29 (2014)
2. Labrie, F., et al.: Screening decreases prostate cancer death: first analysis of the 1988 Quebec prospective randomized controlled trial. Prostate **38**, 83–91 (1999)
3. Durkan, G.C., et al.: Improving prostate cancer detection with an extended-core transrectal ultrasonography-guided prostate biopsy protocol. BJU Int. **89**(1), 33–39 (2002)
4. Imani, F., et al.: Augmenting MRI transrectal ultrasound guided prostate biopsy with temporal ultrasound data: a clinical feasibility study. Int. J. Comput. Assist. Radiol. Surg. **10**, 727–735 (2015)
5. Correas, J.M., et al.: Ultrasound elastography of the prostate: state of the art. Diagn. Interv. Imaging **94**(5), 551–560 (2013)
6. Imani, F., et al.: Computer-aided prostate cancer detection using ultrasound RF time series: *in vivo* feasibility study. IEEE Trans. Med. Imaging **34**(11), 2248–2257 (2015)
7. Duric, N., et al: Whole breast tissue characterization with ultrasound tomography. In: SPIE Medical Imaging (2015)
8. Fincke, J.R., et al: Towards ultrasound travel time tomography for quantifying human limb geometry and material properties. In: SPIE Medical Imaging, San Diego, CA (2016)
9. Huang, L., et al.: Breast ultrasound tomography with two parallel transducer arrays: preliminary clinical results. In: SPIE Medical Imaging, p. 941916 (2015)
10. Aalamifar, F., et al: Co-robotic ultrasound tomography: dual arm setup and error analysis. In: SPIE Medical Imaging (2015)
11. Turkbey, B., et al.: Multiparametric 3T prostate magnetic resonance imaging to detect cancer: histopathological correlation using prostatectomy specimens processed in customized magnetic resonance imaging based molds. J. Urol. **186**(5), 1818–1824 (2011)
12. Negussie, A.H., et al.: Thermochromic tissue-mimicking phantom for optimisation of thermal tumour ablation. Int. J. Hyperth. **32**(3), 239–243 (2016)
13. Aalamifar, F., et al: Image reconstruction for robot assisted ultrasound tomography. In: SPIE Medical Imaging (2016)
14. Tanoue, H., et al: Ultrasonic tissue characterization of prostate biopsy tissues by ultrasound speed microscope. In: Engineering in Medicine and Biology Society (2011)
15. Huthwaite, P., et al.: A new regularization technique for limited-view sound-speed imaging. IEEE Trans. Ultrason. Ferroelectr. Freq. Control **60**(3), 603–613 (2013)